Available online at www.sciencedirect.com
SCIENCE DIRECT
Catalysis Today 116 (2006) 304–312
CATALYSIS TODAY
www.elsevier.com/locate/cattod

Nickel/alumina catalysts modified by basic oxides for the production of synthesis gas by methane partial oxidation

J. Requies [a], M.A. Cabrero [a], V.L. Barrio [a,*], J.F. Cambra [a], M.B. Güemez [a], P.L. Arias [a], V. La Parola [b], M.A. Peña [b], J.L.G. Fierro [b]

[a] School of Engineering (UPV/EHU), Department of Chemical and Environmental Engineering, 48013 Bilbao, Spain
[b] Institute of Catalysis and Petrochemistry, CSIC, Cantoblanco, 28049 Madrid, Spain

Available online 10 July 2006

Abstract

In the present work, Ni/α-Al_2O_3 catalysts modified with different amounts of CaO and MgO were used for the production of hydrogen by catalytic partial oxidation (CPO) and wet-CPO processes of methane. In the wet-CPO process, small additions of water were introduced into the feed of the reactor to improve both the H_2 yield and methane conversion. The addition of water is also beneficial because coke formation becomes thermodynamically unfavorable. The catalysts were characterized before and after the reaction with XRD, XPS, TPR and TPO techniques. Several methane decomposition tests and methane pulse experiments were carried out with a view to correlating the ability of metal sites to activate methane in the absence of oxygen with the performance for CPO and wet-CPO reactions.

Keywords: Magnesium and calcium additives; Catalytic partial oxidation; Nickel catalysts; Catalyst characterization

1. Introduction

The catalytic partial oxidation (CPO) of methane is a process of great interest since it provides a H_2/CO ratio in the product gas close to 2, which is appropriate for methanol synthesis and for the production of synthetic fuels by means of Fischer–Tropsch reactions. In addition, the reaction rate of CPO is much higher – at least one order of magnitude – the conventional steam reforming, thus requiring much smaller reactors.

Non-noble metals such as a nickel [1–4] and cobalt [5] are highly active for CPO but are rapidly deactivated by carbon deposits that form on the catalyst surface and also by the sintering of metal crystallites. An alternative would be the use of noble metal catalysts, because these are less sensitive to carbon deposition [6], although in practice they are not used owing to their high cost. Thus, non-noble metal catalysts are widely used for this type of process, in particular Ni-based ones [1–4]. Several substrates and additives have been used to minimize the extent of coke formation and sintering of metal particles. Catalyst deactivation by coke formation is often a serious drawback in CPO reactions and it has been found that the extent of coke formation depends on the type of nickel species, crystallite size, and the electronic density at the metal site [7]. The incorporation of some additives can alter particle size, the dispersion of the metal on the surface, and the electronic density [8]. The additive may also affect the solid–solid interaction between the oxide catalyst and the support [9], and this influence may be accompanied by significant changes in the catalytic activity of the modified catalyst.

In this work, both Ni/α-Al_2O_3 catalysts and those loaded with small amounts of MgO and CaO were prepared and tested in CPO and wet-CPO reactions. Since the acidity of the support is detrimental to coke formation [10], basic oxides are usually incorporated to neutralize acid sites. Accordingly, this work was undertaken with the aim of analyzing the effects of different additives incorporated to a base Ni/Al_2O_3 catalyst on stability to coke deactivation during the reaction. CaO and MgO additives were selected for this purpose because these basic oxides exhibited good behavior in the analogous CO_2 methane

* Corresponding author. Tel.: +34 946017282; fax: +34 946014179.
E-mail address: laura.barrio@ehu.es (V.L. Barrio).

0920-5861/$ – see front matter
doi:10.1016/j.cattod.2006.05.084

reforming process [11], in which calcium oxide improved the activity and stability of the Ni/α-Al_2O_3 catalysts.

2. Experimental procedure

2.1. Catalyst preparation

An α-Al_2O_3 (BET specific area = 2.5 $m^2\ g^{-1}$, pore volume 0.02 $cm^3\ g^{-1}$, particle size between 0.42 and 0.59 mm) was employed as a support for the catalysts. The catalysts were prepared by the wet impregnation method using Ni$(CH_3COO)_2{\cdot}4H_2O$ as precursor. The α-Al_2O_3 was suspended in a solution containing the required amount of nickel acetate to obtain a nickel content of 15 or 25 wt.% in the final catalyst. The excess of water was evaporated off to dryness in a rotary evaporator at 343 K. The samples were then calcined in air at 1073 K for 4 h.

The Ca- and Mg-modified catalysts were prepared by sequential wet impregnation, following the same procedure as for the Ni/Al_2O_3 sample. The α-Al_2O_3 was first impregnated with Ca or Mg acetate precursor and then dried and calcined at 1073 K for 4 h. Then, nickel was incorporated as described above. A list of the prepared samples is given in Table 1.

2.2. Catalyst characterization

Specific areas were calculated with the BET method from nitrogen adsorption isotherms recorded at 77 K (liquid nitrogen temperature), using a Micromeritics ASAP-2000 apparatus, taking a value of 0.162 nm^2 for the cross-sectional area of the N_2 molecule adsorbed at 77 K. Prior to adsorption measurement, the samples were outgassed at 413 K. The specific area of the catalysts did not differ from the area of the α-Al_2O_3 substrate.

Thermogravimetric analyses were performed on a Mettler Toledo microbalance TGA/SDTA 851. The sample temperature was increased from 323 to 1373 K at 5 K min^{-1} while passing a flow of 20% O_2 in N_2 at a rate of 250 mL(STP) min^{-1}. In the methane pulse experiments, the amount of coke deposited on the used catalysts was underestimated (the sample weight increase due to Ni oxidation was neglected) with this methodology (see Table 7). Gravimetric TPR experiments were also performed using a flow of 20% H_2 in N_2 at a rate of 250 mL(STP) min^{-1}, from 323 to 1373 K at 5 K min^{-1}.

Table 1
Catalysts prepared, nominal composition and NiO crystal size as determined by XRD

Catalysts	Nominal composition	NiO size (nm)
15Ni/Al_2O_3	15.0% Ni	33.0
25Ni/Al_2O_3	25.0% Ni	n.a.
15Ni/Al_2O_3–5Ca	5.0% Ca, 10.0% Ca	22.6
15Ni/Al_2O_3–10Ca	15.0% Ni, 5.0% Mg	n.a.
15Ni/Al_2O_3–5Mg	15.0% Ni, 10.0% Mg	24.6
15Ni/Al_2O_3–10Mg	15.0% Ni	n.a.

n.a.: not available.

Powder X-ray diffraction (XRD) patterns were recorded using a Seifert 3000 P diffractometer, using a nickel filtered Cu $K\alpha_1$ (λ = 0.15406 nm) radiation. The step scans were taken over the range of 2θ angles from 10° to 70°.

A Micromeritics TPD/TPR 2900 apparatus equipped with a TCD was used for temperature-programmed reduction (TPR) analyses. Reduction profiles were obtained by passing a 10% H_2/Ar flow through the samples (sample weight around 50 mg) at a rate of 50 mL(STP) min^{-1}. Temperature was increased from 308 to 1273 K at a rate of 10 K min^{-1} and the amount of hydrogen consumed was determined as a function of temperature.

X-ray photoelectron spectra (XPS) were acquired with a VG Escalab 200R spectrometer equipped with a hemispherical electron analyzer and a Mg Kα ($h\nu$ = 1253.6 eV) X-ray source. The peaks were fitted with a non-linear least squares fitting program using a properly weighted sum of Lorentzian and Gaussian component curves after background subtraction according to Shirley. Charging effects of the samples were corrected by referencing all the energies to the Al 2p peak at 74.5 eV.

CH_4 temperature-programmed decomposition and CH_4 pulse experiments were performed on catalyst samples (50 mg) loaded in a U-shaped quartz reactor connected to a Baltzer Prisma QMS 200 TM quadrupole mass spectrometer. Prior to being tested in the reaction, the catalysts were reduced in a 10% H_2/Ar flow while heating from room temperature up to the temperature was reached at which total metal reduction was achieved (as indicated by TPR experiment) and then left at this temperature for 30 min. Following this, the reactor was cooled down to room temperature in an Ar flow and finally a flow of 10% of CH_4/Ar (150 mL min^{-1}) was passed while heating to 1123 K (10 K min^{-1}) for the decomposition experiment. The procedure employed in the pulse experiments was different: the samples were heated up to 1123 K in an Ar flow and then exposed to pulses (0.1 mL) of 10% CH_4/Ar mixture. In both cases, the signals of H_2, H_2O, CH_4, CO, CO_2 and Ar were recorded. In order to eliminate errors due to possible flow variations all signals were referred to the Ar signal.

2.3. Activity measurements

The experiments were conducted at atmospheric pressure in a bench-scale unit using a steel fixed-bed catalytic reactor. The reactor (1.15 cm i.d. and 30 cm length) was heated electrically in a furnace. The effluent stream was cooled down, thus water was collected and weighted, and the gas phase was analyzed on-line by a GC (HP5890) equipped with FID and TCD detectors. Two columns, Porapak Q and Molecular Sieve 5A, were used in a series/bypass arrangement for the complete separation of H_2, CH_4, CO and CO_2. Activity measurements were carried out in the CPO of methane, under atmospheric pressure at 1073 K with a feed of $CH_4/O_2/N_2$ = 2/1/3.8 (molar ratio). The catalyst weight (180 mg) was diluted with SiC at a 1:9 ratio to avoid temperature variations in the bed. The particle size range was between 0.42 and 0.59 mm. For wet-CPO tests, the steam/carbon ratio (S/C) was increased from 0 to 0.6. For some

Table 2
Activity tests for the Ca- and Mg-promoted catalysts and for 15% Ni–Al_2O_3 and the 25% Ni–Al_2O_3 catalysts at WHSV = 600 and 800

Catalysts	CH_4 conversion (%), 95.1[a]		H_2 yield, 1.87[a]		H_2 selectivity (%), 98.3[a]		CO selectivity (%), 98.2[a]		M, 1.95[a]	
	600[b]	800[b]	600[b]	800[b]	600[b]	800[b]	600[b]	800[b]	600[b]	800[b]
15Ni/Al_2O_3	88.9	85.8	1.60	1.45	93.9	93.1	95.1	91.7	1.80	1.71
25Ni/Al_2O_3	91.6	91.6	1.68	1.70	94.0	93.9	95.3	94.6	1.81	1.78
15Ni/Al_2O_3–5Ca	92.7	93.1	1.78	1.75	94.1	94.1	96.3	96.0	1.84	1.84
15Ni/Al_2O_3–10Ca	92.0	91.5	1.65	1.63	94.0	93.9	95.5	94.3	1.81	1.77
15Ni/Al_2O_3–5Mg	93.5	94.4	1.74	1.74	94.1	94.1	96.1	95.9	1.83	1.82
15Ni/Al_2O_3–10Mg	92.6	92.7	1.69	1.65	94.1	94.0	96.4	95.8	1.84	1.80

[a] Equilibrium data.
[b] WHSV (g_{feed}/g_{cat} h).

experiments the O_2/CH_4 ratio was decreased to 0.4 and the pressure was changed to 3 bar (with 240 mg of catalyst and the same dilution). Prior to the tests, the catalysts were pre-reduced *in situ* at 1073 K at atmospheric pressure in an H_2/N_2 mixture of 270 mL(STP) min^{-1} (3:1, v/v) for 3.5 h. After catalyst activation, activity measurements were performed, varying WHSV between 600 and 1200 h^{-1} ($g_{gas}\, g_{cat}^{-1}\, h^{-1}$). The reaction was kept running for each space velocity until steady-state was reached.

For a better understanding of the catalytic activity and the product distribution, the following parameters were calculated:

- Methane conversion: $CH_4\,\text{conversion}\,(\%) = 100 \times ((F_{CH_4}^{feed} - F_{CH_4}^{out})/F_{CH_4}^{out})$;
- Hydrogen selectivity: $H_2\,\text{selectivity}\,(\%) = 100 \times (F_{H_2}^{out}/(F_{H_2}^{out} + F_{H_2O}^{out}))$;
- Hydrogen yield: $H_2\,\text{yield} = F_{H_2}^{out}/F_{CH_4}^{feed}$;
- CO selectivity: $CO\,\text{selectivity}\,(\%) = 100 \times (F_{CO}^{out}/(F_{CO}^{out} + F_{CO_2}^{out}))$;
- M parameter: $M = (F_{H_2}^{out} - F_{CO_2}^{out})/(F_{CO_2}^{out} + F_{CO}^{out})$.

M is a useful parameter that determines the suitability of the syngas produced in the Fischer–Tropsch process. In this process, feeds containing significant amounts of CO_2 are not desirable, and hence M values of around 2.1 are of interest. Finally, the corresponding values for the thermodynamic equilibrium corresponding to reaction conditions were plotted in order to compare them with the experimental results obtained.

3. Results and discussion

3.1. Catalytic activity

3.1.1. Evaluation of the Ca- and Mg-supported catalysts activity in CPO

Tables 2 and 3 show the activity of the Ca-modified catalysts for different space velocities. The activity of the 15% and 25% Ni is also shown for comparative purpose. The activity of the Ca-modified catalysts increased slightly on increasing the weight hourly space velocity (WHSV) from 600 to 800 h^{-1} while it decreased for higher space velocities. For the lowest space velocity, transport limitations might be involved. For WHSV = 800 h^{-1}, the activity of the 5% Ca-containing catalyst increases up to 93% (see Table 2). Increasing the Ca content up to 10% did not seem to enhance CH_4 conversion any more. The H_2 yield and the CO selectivity also increase upon Ca incorporation, while the M value reaches 1.84, somewhat lower than the optimum one for FT application. The same trend can be observed in Tables 2 and 3 for the Mg-loaded catalysts. As occurred with the Ca-modified catalysts, the addition of Mg increased methane conversion up to 93–94%, although no significant differences in activity were observed upon increasing the Mg content from 5 to 10%.

Table 3
Activity tests for the Ca- and Mg-promoted catalysts and for 15% Ni–Al_2O_3 and the 25% Ni–Al_2O_3 catalysts at WHSV = 1000 and 1200

Catalysts	CH_4 conversion (%), 95.1[a]		H_2 yield, 1.87[a]		H_2 selectivity (%), 98.3[a]		CO selectivity (%), 98.2[a]		M, 1.95[a]	
	1000[b]	1200[b]	1000[b]	1200[b]	1000[b]	1200[b]	1000[b]	1200[b]	1000[b]	1200[b]
15Ni/Al_2O_3	77.3	72.7	1.28	1.13	89.7	87.8	87.2	81.9	1.60	1.46
25Ni/Al_2O_3	86.2	83.9	1.56	1.50	93.6	93.5	92.5	91.6	1.73	1.71
15Ni/Al_2O_3–5Ca	88.2	83.1	1.64	1.50	93.8	93.5	94.1	91.6	1.78	1.71
15Ni/Al_2O_3–10Ca	79.4	79.3	1.36	1.34	89.5	91.0	88.5	88.5	1.61	1.62
15Ni/Al_2O_3–5Mg	89.7	84.2	1.64	1.47	93.9	92.6	94.3	91.5	1.79	1.69
15Ni/Al_2O_3–10Mg	88.1	85.6	1.55	1.49	93.8	92.7	93.9	92.6	1.76	1.74

[a] Equilibrium data.
[b] WHSV (g_{feed}/g_{cat} h).

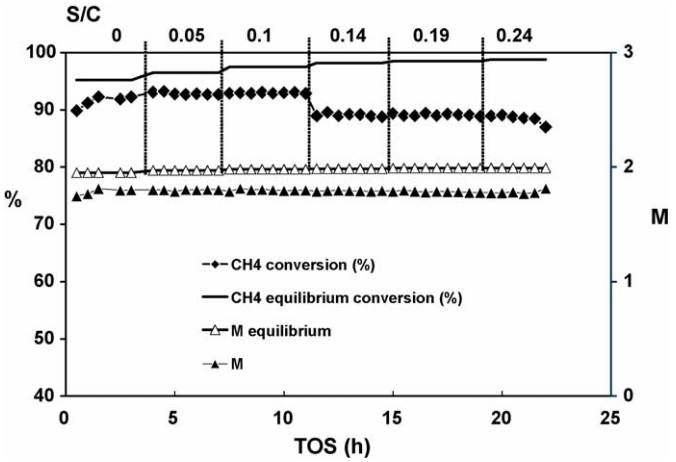

Fig. 1. Wet-CPO activity test of the 15% Ni/Al_2O_3–10Ca catalyst with S/C = 0–0.24 and O_2/CH_4 = 0.5 at 1073 K and P = 1 bar (WHSV = 600 h^{-1}).

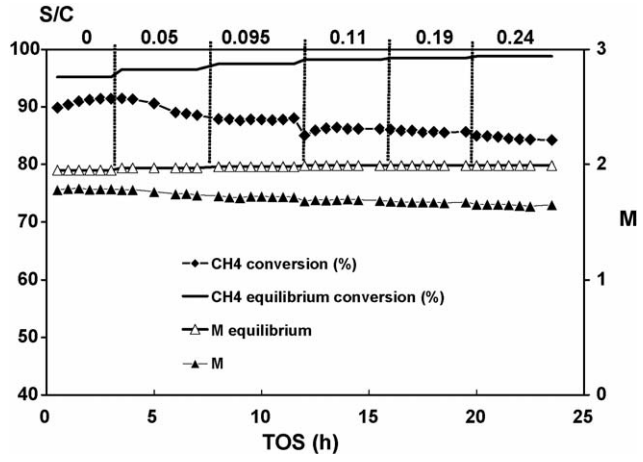

Fig. 2. Wet-CPO activity test of the 15% Ni/Al_2O_3–10Mg catalyst with S/C = 0–0.24 and O_2/CH_4 = 0.5 at 1073 K and P = 1 bar (WHSV = 600 h^{-1}).

3.1.2. *Influence of the S/C and O_2/CH_4 ratios on the activity of Ca- and Mg-modified catalysts*

From thermodynamic predictions, a further increase in both methane conversion and value of M parameter could be achieved by adding water into the feed. For the non-doped Ni catalyst, activity decreased strongly until values of 70% for an S/C ratio of 0.2. Fig. 1 shows the behavior of the 10% Ca-doped catalyst. For S/C ratios lower than 0.1, activity did not change whereas both activity and CO and H_2 selectivities decreased for higher S/C ratios. On the other hand, the M value remained close to 1.8. In another set of experiments, as well as steam addition the oxygen feed was decreased trying to force the steam reaction to occur. Thus, several experiments were carried out, varying the S/C ratio while decreasing the O_2/CH_4 ratio to 0.4. For all S/C ratios, methane conversion decreases and the M value approached 1.9.

The addition of steam to the feed mixture did not enhance the activity of the 10% Mg-loaded catalyst (see Fig. 2). Similarly, for an O_2/CH_4 ratio of 0.4 methane conversion fell markedly to 77% and remained almost unchanged on increasing the S/C ratio. Despite the thermodynamics prediction of higher methane conversion at lower O_2/CH_4 ratios, catalyst activity decreased upon increasing the S/C ratio.

3.1.3. *Further activity tests for the promoted catalysts*

This third set of activity experiments included study of the steam content in CH_4 conversion over Ca- and Mg-loaded catalysts at higher pressures. Table 4 summarizes CPO and wet-CPO activities at 1073 K and 3 bar. For the 10% Ca-containing catalysts, CH_4 conversion decreases slightly (from 87.6 to 81.4%) upon increasing the S/C ratio from 0 to 0.1. Nevertheless, it increased again to 88.2% (see Table 4) for a S/C ratio of 0.2, which is somewhat higher than that reached in the absence of steam in the feed. In addition, CO and H_2 selectivities decreases, the M value remained constant and the H_2 yield increased for higher S/C ratio. A similar kind of behavior was found for the 5% Ca-loaded catalyst.

The Mg-loaded catalysts behaved similarly to the Ca-containing counterparts. The activity of the 10% Mg-containing catalyst decreased slightly for an S/C ratio of 0.1 (Fig. 3) and then increased up to 93.2% for an S/C ratio of 0.2. Similarly, the H_2 yield increased significantly from 1.73 to 1.91 (Table 4). It was also observed that activity was slightly higher for the 10% Mg-loaded catalyst than for the 5% Mg-loaded counterpart. For the two most promising catalysts, containing 10% Ca and 10% Mg, the S/C ratio was increased until higher ratios. The results shown in Table 5 indicate that the activity of the Ca-loaded catalyst did not increase any further for higher S/C ratios. In contrast, in the case of the Mg-loaded catalyst activity increases up to an S/C ratio of 0.4 and remained nearly constant for higher S/C ratios (96.3–96.5%). It was also noted that H_2 and CO selectivities decreases, but the H_2 yield increased to 2.0, due to the higher conversion achieved. Finally, temperature was also

Table 4
CPO and wet-CPO activity for the Ca- and Mg-promoted catalysts with S/C ratios from 0 to 0.2 at 1073 K and P = 3 bar (O_2/CH_4 = 0.5)

	Catalysts											
	5Ca			10Ca			5Mg			10Mg		
	0[a]	0.1[a]	0.2[a]	0[a]	0.1[a]	0.2[a]	0[a]	0.1[a]	0.2[a]	0[a]	0.1[a]	0.2[a]
CH_4 conversion (%)	88.6	81.3	89.4	87.6	81.4	88.2	89.6	81.0	90.0	90.9	87.3	93.2
CO selectivity (%)	96.8	87.9	89.1	96.1	88.6	89.0	96.5	85.3	88.0	96.7	92.8	91.2
H_2 selectivity (%)	97.2	92.5	91.5	96.6	90.4	91.0	97.5	90.1	91.1	97.7	94.8	93.2
H_2 yield	1.70	1.55	1.76	1.63	1.52	1.73	1.69	1.46	1.72	1.73	1.77	1.91
M	1.85	1.73	1.83	1.82	1.72	1.82	1.84	1.70	1.80	1.84	1.83	1.88

[a] S/C ratio.

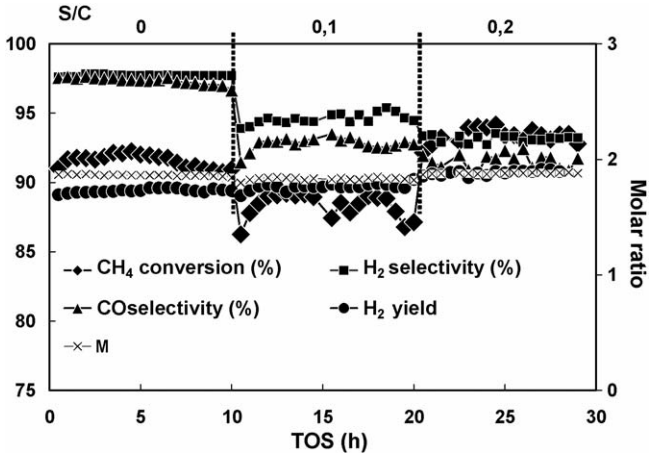

Fig. 3. Wet-CPO activity tests of activity of the 15% Ni/Al_2O_3–10Mg catalyst with S/C = 0–0.2 at 1073 K and P = 3 bar (WHSV = 600 h^{-1}).

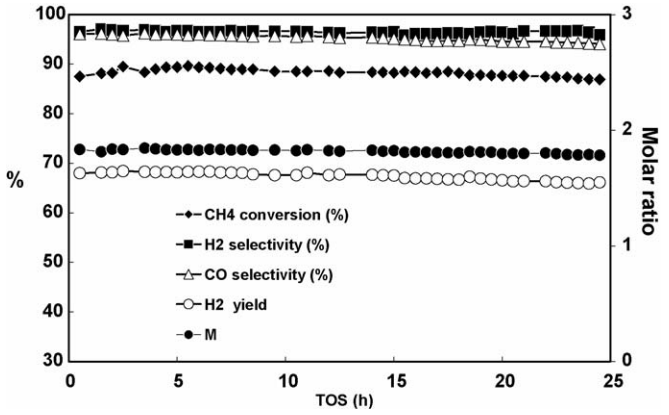

Fig. 4. Long-term activity test for the CPO reaction of the 15%Ni/Al_2O_3–10Mg catalyst at 1073 K and P = 3 bar (F/W = 600 h^{-1}).

increased from 1073 to 1123 K; the results are shown in Table 5. As expected, methane conversion increased up to 96.9%.

For the 15% Ni (Al_2O_3–10Mg) catalyst, which showed the highest methane conversion and H_2 yield, a long-term activity test by the CPO reaction was performed. The results at 1073 K and 3 bar are shown in Fig. 4. As can be observed, activity remained stable for the time on-stream operated (TOS = 25 h).

3.2. Catalyst characterization

3.2.1. X-ray diffraction

The X-ray diffraction patterns of the calcined catalysts (Fig. 5) show diffraction peaks due to α-Al_2O_3 (pdf 73-1512) and NiO (pdf 47-1049). For the Ca-loaded samples, diffraction lines of CaO (pdf 77-2010) were also observed. The pattern of the Mg-doped sample was more complex because the diffraction lines of NiO overlapped with those of MgO (pdf 78-0430), although the relative intensity ratio of the NiO and MgO phases was different, and a mixed Ni–Mg oxide $Mg_{0.4}Ni_{0.6}O$ (pdf 34-0410) displayed the same diffraction lines and peak ratios as NiO. The fact that the peaks at 37.2, 43.3 and 62.9 2θ were shifted slightly towards lower diffraction angles (see inset in Fig. 5) could be taken as an indication of the formation of the mixed Ni–Mg–O phase. In addition, the Mg-loaded sample displayed small peaks at 44.4 and 65.2° which are characteristic of the nickel aluminate phase (pdf 81-0722). An estimate of the particle sizes of the NiO phase was made by measuring the line broadening of the most intense reflection line and applying Sherrer's equation. The particle sizes calculated were between 23 and 40 nm (Table 1).

3.2.2. Temperature-programmed reduction (TPR)

The temperature-programmed reduction profiles of the catalysts are shown in Figs. 6 and 7. The profile of the alumina-supported Ni sample is typical of NiO weakly interacting with the alumina substrate [12]. The low temperature peak (679 K) can be attributed to the NiO bulk or weakly interacting with the support. The reduction temperature of bulk NiO is 650 K, which is substantially lower than that (805 K) arising from the reduction of so-called ''fixed NiO'' species. The calcium-loaded sample showed a complex profile with several components spread over a wide temperature range. Calcium carbonate species developed on this sample contributed to this complexity. On conducting the TPR measurements in a microreactor connected on-line with a mass spectrometer, methane and carbon monoxide were detected along the reduction process. The appearance of these species can be explained in terms of the reduction and/or thermal decomposition of calcium carbonates. The magnesium-loaded sample

Table 5
Wet-CPO activity for the 10% Ca and 10% Mg-promoted catalyst with S/C ratios from 0.3 to 0.6 at 1073 K and P = 3 bar (O_2/CH_4 = 0.5)

	Catalysts						
	10Ca		10Mg				
	0.3[a]	0.4[a]	0.3[a]	0.4[a]	0.5[a]	0.6[a]	0.4[a,b]
CH_4 conversion (%)	84.8	84.9	94.7	96.3	96.5	96.3	96.9
CO selectivity (%)	87.3	84.7	93.6	86.1	83.0	80.1	87.6
H_2 selectivity (%)	83.5	80.3	91.9	88.4	85.6	83.8	88.1
H_2 yield	1.71	1.71	1.83	1.93	2.00	1.99	1.96
M	1.75	1.75	1.88	1.86	1.85	1.84	1.88

[a] S/C ratio.
[b] At 1123 K.

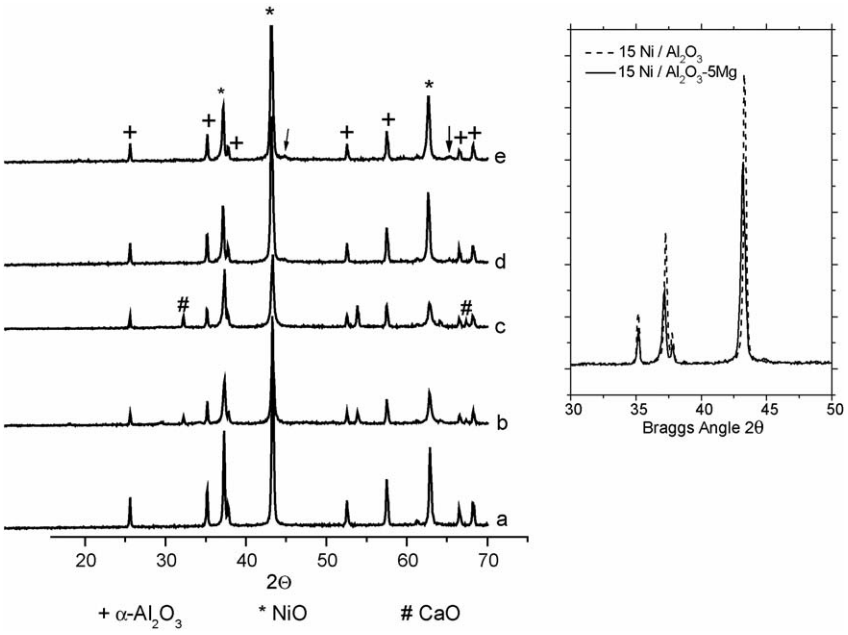

Fig. 5. X-ray diffraction patterns of the calcined catalysts: (a) 15Ni/Al_2O_3; (b) 15Ni/Al_2O_3–5Ca; (c) 15Ni/Al_2O_3–10Ca; (d) 15Ni/Al_2O_3–5Mg; (e) 15Ni/Al_2O_3–10Mg. Inset: zoom in the 30–50° 2θ range for the 15Ni/Al_2O_3 and 15Ni/Al_2O_3–5Mg catalysts.

showed reduction peaks at higher temperature (1058 and 1254 K), and the intensity of the high temperature peak increased at higher magnesium loading. These peaks might arise from nickel–magnesium mixed oxide or from nickel aluminate [13–15]. It is clear that no trace of ''free NiO'' was present in this sample.

3.2.3. Photoelectron spectroscopy

The XPS results are summarized in Table 6. Both the Ni $2p_{3/2}$ binding energy and the full width at half maximum (FWHM) are invariant with the support composition, indicating that the chemical state was the same and for all samples. Even though the values in the literature for the Ni 2p binding energies are spread over a fairly broad energy interval [16–20], the value of 855.5 eV (±0.3 eV) can be assigned to NiO. Moreover, the Ni $2p_{5/2}$–Ni $2p_{3/2}$ splitting of 17.7 eV confirms this assignment [16], and the presence of strong shake-up satellite structures indicates the presence of Ni(II) ions in a paramagnetic state. It is noteworthy that the FWHM was quite large (−3.8 ± 0.1 eV versus 1.8 eV of pure NiO), indicating a surface heterogeneity of the supported nickel, which is exposed in different environments, from the ''free NiO'' to the NiO interacting strongly with the support.

The Ni/Al intensity ratios (see Table 6) indicate that the surface dispersion of nickel increased in the 5 wt.% Ca- and 5 wt.% Mg-loaded samples, and particularly so in the latter, which showed a better nickel surface dispersion. The Ni/Al ratio values did not increase further when the Ca and Mg

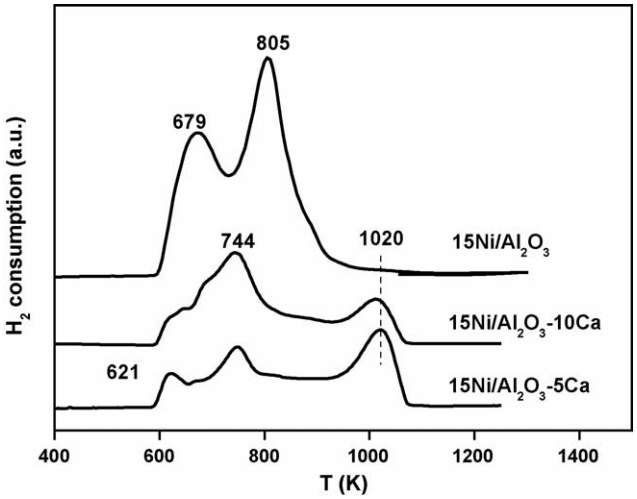

Fig. 6. TPR profile of the 15% Ni catalyst and for 5 and 10% Ca-loaded catalysts.

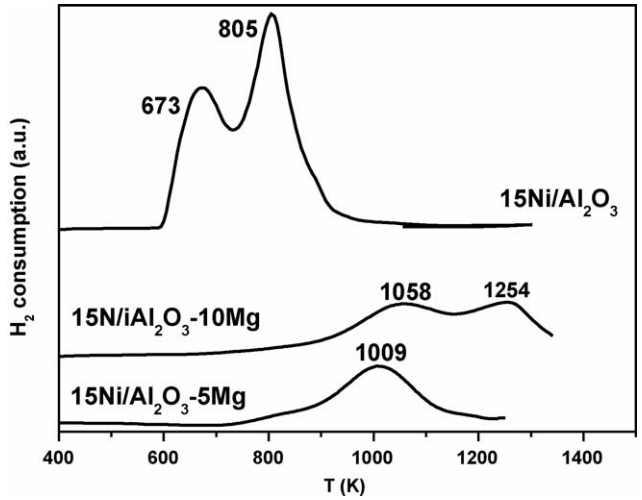

Fig. 7. TPR profile for the 15% Ni catalyst and for 5 and 10% Mg-doped catalysts.

Table 6
Binding energies, relative percentages and Ni/Al intensity ratio of calcined samples

Catalysts	Ni $2p_{3/2}$	O 1s	C 1s	Ni/Al
$15Ni/Al_2O_3$	855.4 (3.9)	530.4 (2.5) 69%, 532.1 (2.3) 31%	285.7 (2.5), 289.3 (3.0)	0.9
$15Ni/Al_2O_3$–5Ca	855.6 (3.8)	531.3 (2.8) 81%, 532.6 (1.9) 19%	285.5 (2.3), 290.1 (2.0)	1.3
$15Ni/Al_2O_3$–10Ca	855.9 (3.8)	530.4 (2.2) 18%, 532.4 (2.4) 82%	285.5 (2.3), 290.1 (2.0)	0.7
$15Ni/Al_2O_3$–5Mg	855.9 (3.6)	530.7 (2.6) 81%, 532.7 (1.9) 19%	285.6 (2.2), 289.9 (2.9)	2.0
$15Ni/Al_2O_3$–10Mg	856.0 (3.3)	530.6 (2.1) 15%, 532.4 (2.1) 85%	285.7 (2.2), 289.3 (3.3)	1.3

In parenthesis, FWHM.

additives were increased up to 10%. Additionally, the Ni/Al ratio of the Ca-loaded sample was lower than that of the Ca- and Mg-free counterparts. The C 1s peak (see Fig. 8) revealed the component of adventitious carbon at 285 ± 0.2 eV and also a peak at a higher binding energy (−289.5 ± 0.5 eV), attributed to surface carbonates [21]. This latter peak was particularly intense in the Ca-loaded catalyst and was hardly detected in the Mg-loaded one.

3.2.4. Methane decomposition and surface carbon

The methane thermal decomposition profiles over the various samples are shown in Fig. 9. Thermal decomposition of methane produces H_2, which evolves and is detected by a mass spectrometer, and carbon which stays on the surface. The non-doped catalyst ignites methane decomposition at −650 K and the decomposition persists up to 1100 K with two clear peaks: an intense peak at 800 K and a less intense and broad one at 930 K. The methane decomposition profiles of the Ca- and Mg-loaded samples are very similar, with a maximum at 780 K. The Mg-containing sample formed much more H_2 than the Ca-loaded one, indicating a higher capacity for methane decomposition. The area below the H_2 evolution curves is shown in Table 7. Thermal programmed oxidation (TPO) analysis of the fresh and used catalysts in the methane decomposition experiments afforded very similar results for the different catalysts, indicating that examination of the combustion of the surface carbon does not permit differences between

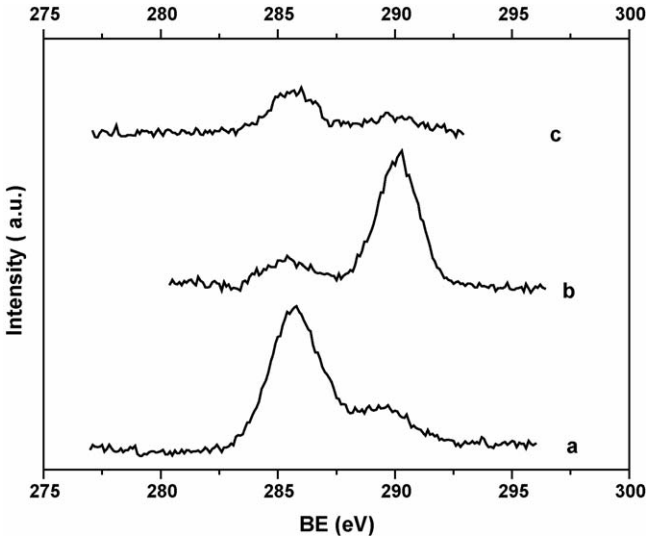

Fig. 8. XPS C 1s level of calcined catalysts: (a) $15Ni/Al_2O_3$; (b) $15Ni/Al_2O_3$–5Ca; (c) $15Ni/Al_2O_3$–5Mg.

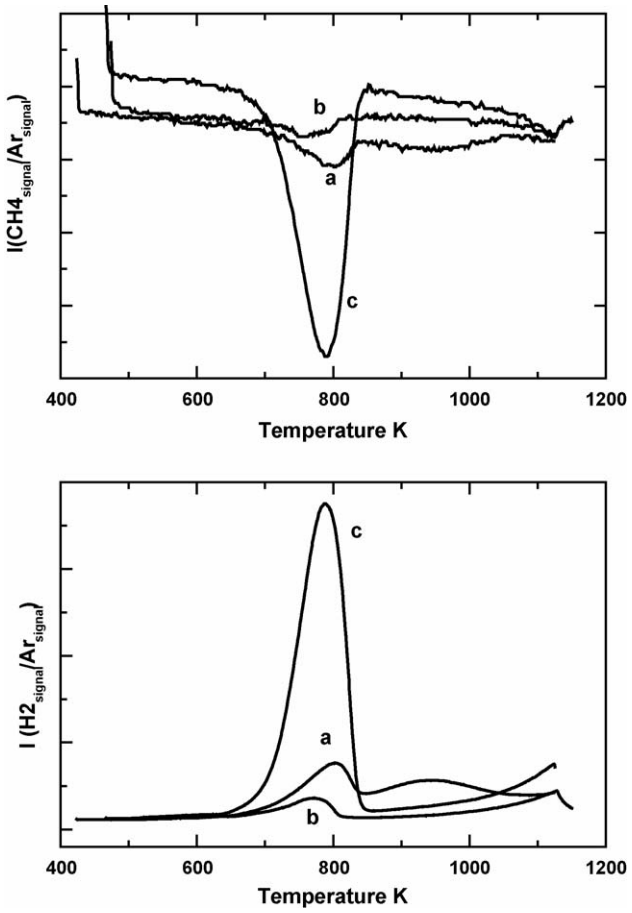

Fig. 9. Methane thermal decomposition and hydrogen evolution over the reduced catalysts: (a) $15Ni/Al_2O_3$; (b) $15Ni/Al_2O_3$–5Ca; (c) $15Ni/Al_2O_3$–5Mg.

α- and β-carbon to be established. After TPO and the subsequent removal of the surface carbon and nickel re-oxidation, gravimetric TPR experiments were carried out on these used catalysts. Fig. 10a shows the derivative of the TPR weight loss corresponding to the catalysts used in the CPO

Table 7
Carbon deposited over catalysts after 72 h of reaction, methane decomposition and methane pulses

Catalysts	After 72 h on stream	After CH_4 decomposition		After CH_4 pulses
$15Ni/Al_2O_3$	$C = 8.8\%$	$C = 7.8\%$	$A_{H_2} = 0.84$	$C = -0\%$
$15Ni/Al_2O_3$–5Ca	$C = 10.4\%$	$C = 3.6\%$	$A_{H_2} = 0.31$	$C = 2.6\%$
$15Ni/Al_2O_3$–5Mg	$C = 3.1\%$	$C = 19.0\%$	$A_{H_2} = 1.84$	$C = 1.6\%$

Area below the H_2 evolution curves due methane decomposition.

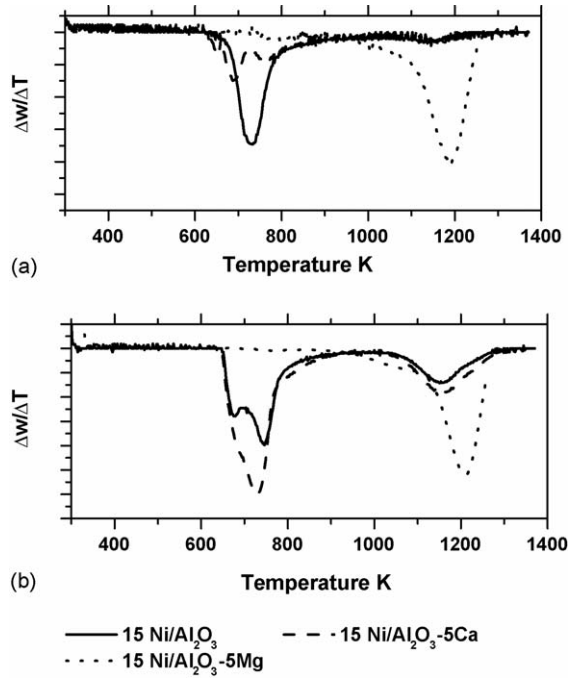

Fig. 10. Derivative of the thermogravimetric TPR after TPO of used catalysts (a) used in CPO of methane at 1073 K; (b) used in methane decomposition at 1123 K.

reaction and Fig. 10b shows the equivalent experiment for the catalysts used in methane decomposition at 1123 K. The TPR profiles of Mg-loaded catalyst were very similar to that of the fresh catalyst (Fig. 7), with reduction peaks at high temperature due to the presence of Ni–Mg–O oxide and nickel aluminate. Nevertheless, it is interesting to note the behavior of the Ca-doped catalysts. First, the reduction of the surface carbonates detected in the TPR of fresh catalysts (Fig. 6) disappeared since previous oxidation treatments had been performed (TPO). In addition, only the reduction component due to NiO interacting strongly with the support was observed, with no signal of ''free NiO''. A component at high temperature (1150 K), due to the formation of nickel aluminate, also appeared in both Ca-free and Ca-loaded catalysts. This component had low intensity in the catalysts used in the CPO reaction, but it was very clear for the catalyst used in methane decomposition. Therefore, an important change must occur in the structure of the nickel species of the Ca-free and Ca-loaded catalysts due to modification of the nickel-support interaction during the reaction. Notwithstanding, the structure of Mg-loaded catalysts was more stable than that of the Ca-counterparts.

The pulse experiments over the reduced catalysts are shown in Fig. 11. Comparison of the catalysts behavior is very interesting. Methane consumption in the first pulse was quite high in both the modified and unmodified catalysts, and was accompanied by H_2 and CO formation. However, the behavior of the catalyst differed in ensuing pulses. In the second pulse,

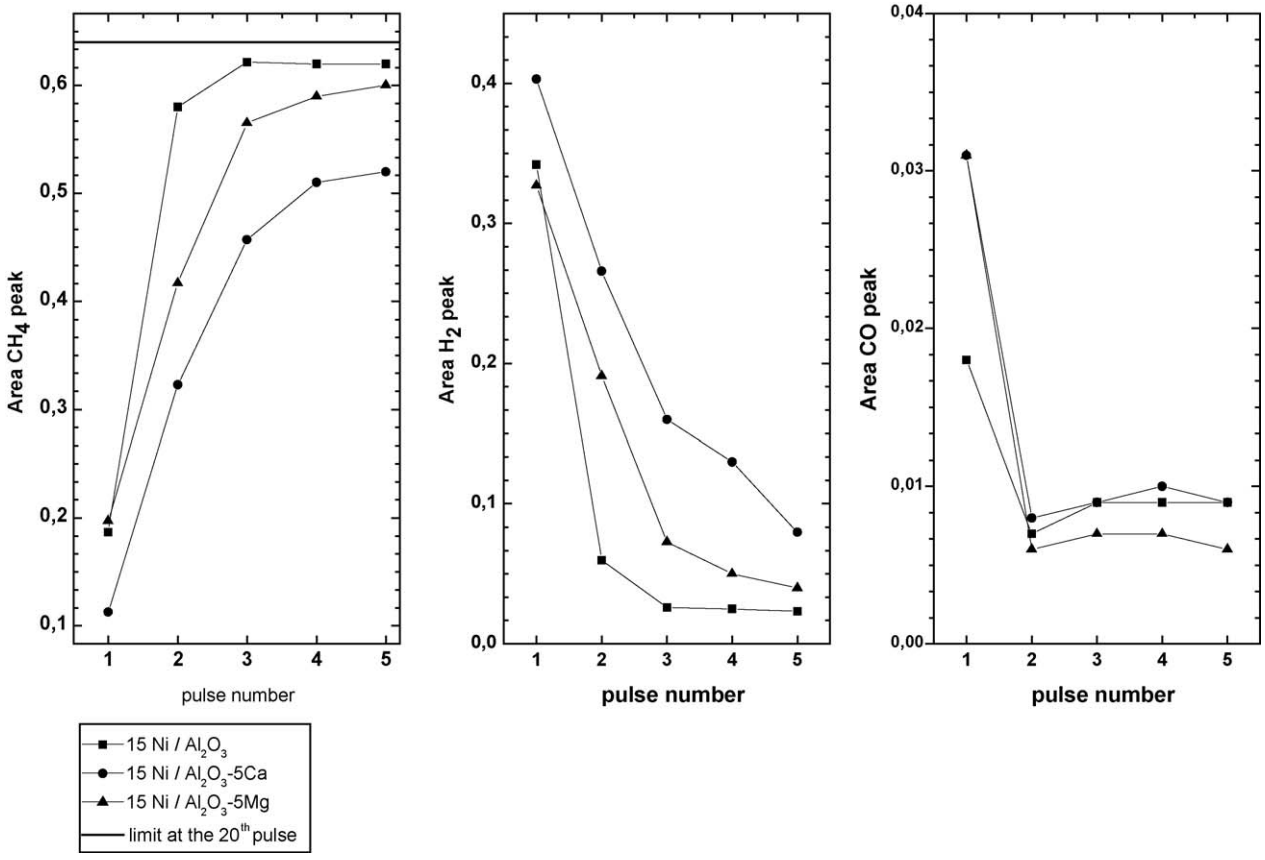

Fig. 11. Methane pulse experiments over the reduced catalysts.

both CH_4 conversion and H_2 selectivity over the unmodified catalyst were strongly inhibited. In contrast, the modified catalysts displayed a higher CH_4 conversion and H_2 production. Additional pulses showed some stabilization in CH_4 conversions for all the catalysts. The Ca-doped one remains the most active after five pulses. Nevertheless, almost no CO production was observed after the first pulse in either the modified or unmodified catalysts and as a result the C must remain accumulated on the catalyst surface. These observations are in agreement with the amounts of coke accumulated on the surface after the methane pulses (Table 7).

Pulse experiments were performed in the absence of oxygen in the feed stream. Accordingly, in this set of experiments any methane oxidation must be attributed to some oxygen released by the support. It should be noted that the amount of oxygen donated by the alumina substrate is very low and only occurs in the first pulse [22], and this is accounted for by the formation of CO only in the first pulse. Pulse experiments revealed that the ability of the modified and unmodified catalysts to release oxygen from the catalyst structure was very similar (first pulse). Therefore, the differences in the CPO activity cannot be correlated with the activity of the bulk oxygen (it must be also consider that the CPO activity tests were all performed at 1073 K). Differences could only be established along successive methane pulses, when no oxygen was available and methane conversion was only occurring by means of the decomposition step. In these pulses, the modified catalysts maintained some activity, and this should be attributed to the presence of active sites for the decomposition of methane in the absence of oxygen.

4. Conclusions

Modification of Ni/Al_2O_3 catalysts by Ca- and Mg-additives improves the performance in CPO reactions. For the Ca- and Mg-modified catalysts, a higher Ni dispersion and a lower carbon deposition (as measured by XPS in the CPO activity tests used samples) and sintering were observed. Characterization analysis of the used catalysts revealed that the structure of the nickel species in Mg-loaded catalysts was more stable than in the Ca-modified and unmodified catalysts. Nevertheless, the improvement in catalytic activity of the Mg- and Ca-modified catalysts could be related to the presence of active sites for the decomposition of methane in the absence of oxygen.

Acknowledgements

The authors gratefully acknowledge the financial support of this work by the European Union (V Framework Program, LTCPO-GTL No. NNE5-2002-00424) and the University of the Basque Country.

References

[1] F. Basile, L. Basini, M. D'Amore, G. Fornasari, A. Guarinoni, D. Matteruzzi, G. del Piero, F. Trifiro, A. Vaccari, J. Catal. 173 (1998) 247.
[2] H. Provendier, C. Petit, C. Estournès, S. Lisbs, A. Kiennemann, Appl. Catal. A: Gen. 180 (1999) 163.
[3] C.J. Michael, M. Bradford, Albert Vannice. Catal. Today 50 (1999) 87.
[4] N.N. Nichio, M.L. Casella, G.F. Santori, E.N. Ponzi, O.A. Ferretti, Catal. Today 62 (2000) 231.
[5] H.Y. Wang, E. Ruckenstein, J. Catal. 199 (2001) 309.
[6] J.R. Rostrup-Nielsen, J.H.B. Hansen, J. Catal. 144 (1993) 38.
[7] J.R. Rostrup-Nielsen, in: J.R. Anderson, M. Boudart (Eds.), Catalysis, Science and Technology, vol. 5, Springer, Berlin, 1984, pp. 1–117.
[8] E. Ruckenstein, Y.H. Hu, Catal. Rev. Sci. Eng. 44 (2002) 423.
[9] J. Houalla, B. Lemaitre, Delmon, J. Chem. Soc., Faraday Trans. 78 (1982) 1389.
[10] Z. Hou, O. Yokota, T. Tanaka, T. Yashima, Appl. Catal. A: Gen. 253 (2003) 381.
[11] S. Cavallaro, S. Freni, G. Calogero, J. Power Sources 87 (2000) 28.
[12] J.M. Rynkowski, T. Paryjczak, M. Lenik, Appl. Catal. A: Gen. 106 (1993) 73.
[13] T. Shishido, M. Sukenobu, H. Morioka, M. Kondo, Y. Wang, K. Takaki, K. Takehira, Appl. Catal. A: Gen. 223 (2002) 35.
[14] J.T. Richardson, B. Turk, M.V. Twigg, Appl. Catal. A: Gen. 148 (1996) 97.
[15] W. Chu, W. Yang, L. Lin, Appl. Catal. A: Gen. 235 (2002) 39.
[16] B.W. Hoffer, A.D. van Langeveld, J.P. Janssens, R.L.C. Bonné, C.M. Lok, J.A. Moulijn, J. Catal. 192 (2003) 432.
[17] F. van Looij, J.W. Geus, J. Catal. 168 (1997) 154.
[18] H. Morioka, Y. Shimizu, M. Sukenobu, K. Ito, E. Tanabe, T. Shishido, K. Takehira, Appl. Catal. A: Gen. 215 (2001) 11.
[19] Z. Hou, O. Yokota, T. Tanaka, T. Yashima, Appl. Catal. A: Gen. 253 (2003) 381.
[20] A.A. Lemonidou, M.A. Goula, I.A. Vasalos, Catal. Today 46 (1998) 175.
[21] C.S. Gopinath, S.G. Hegde, A.V. Ramaswamy, S. Mahapatra, Mater. Res. Bull. 37 (2002) 1323.
[22] K.H. Hofstad, J.H.B.J. Hoebink, A. Holmen, G.B. Marin, Catal. Today 40 (1998) 157.